NASA TN D-1813

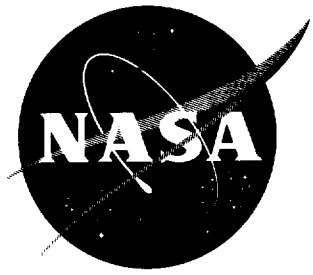

TECHNICAL NOTE

D-1813

A STATISTICAL MODEL FOR SYNTHETIC WIND PROFILES FOR AEROSPACE VEHICLE DESIGN AND LAUNCHING CRITERIA

By Robert M. Henry

Langley Research Center
Langley Station, Hampton, Va.

NATIONAL AERONAUTICS AND SPACE ADMINISTRATION

WASHINGTON July 1963

NATIONAL AERONAUTICS AND SPACE ADMINISTRATION

TECHNICAL NOTE D-1813

A STATISTICAL MODEL FOR SYNTHETIC WIND PROFILES FOR AEROSPACE VEHICLE DESIGN AND LAUNCHING CRITERIA

By Robert M. Henry

SUMMARY

A model for extreme-value wind-velocity profiles based on the multivariate Gaussian (joint normal) distribution of the horizontal components of wind velocity is presented. These profiles can be constructed rapidly and objectively wherever the parameters of the wind distribution are known, and they can be tailored to a specific location, season, launch azimuth, and critical altitude. Some examples of these profiles are shown and discussed. In addition to the usual design-criterion profile, methods of constructing extreme-value profiles for launching criteria are presented, and the application of these profiles in aerospace vehicle operations is indicated. Derivation of the equations used to construct the profiles and derivation and discussion of confidence limits are presented in appendixes.

INTRODUCTION

The passage of vertically rising vehicles through rapidly varying horizontal winds induces loads and control disturbances which are important to the design and operation of these vehicles. A complete solution of the resulting problems requires treatment of both the large-scale and the small-scale variations of wind with height. The present report treats the large-scale variations (wave lengths greater than about 1 kilometer) which can be derived from standard radiosonde data. No completely satisfactory method of treating the entire spectrum of disturbances has yet been developed, partly because of the lack of adequate data concerning the small-scale variations of the wind with height, and partly because of the mathematical difficulties in the analysis of the response of a nonlinear time-variant system to a nonstationary random input. These problems are under attack (refs. 1 to 5), but it appears that a satisfactory overall solution still lies in the future.

The technique described herein provides an objective method for the efficient utilization of the great amount of large-scale wind data which are now available. Joint normal (Gaussian) distributions fitted to available wind data are used to obtain conditional distributions which define the probability of simultaneous occurrence of extreme wind velocity and extreme wind shear (change of wind with height) for various layer thicknesses. These extreme values are

then combined into a synthetic wind profile which can be used in load or control disturbance calculations.

Advantages of this technique as compared to those previously in use are as follows:

(1) Profiles can be rapidly constructed to fit the special requirements of a particular situation. This is especially important for space systems for which there may be a very limited number of launches of a particular vehicle configuration, and performance may be increased by designing to the particular conditions applying to these launches.

(2) The use of a fitted-model distribution produces more stable estimates of the extremes than empirical methods; that is, they are less likely to be drastically changed by a few additional data. Furthermore, they are less sensitive to large errors in the small number of very large winds.

(3) The use of components rather than magnitudes eliminates a source of overconservatism which is present in all profiles based on the total wind speed. It also permits pitch-plane and cross-range loads to be studied separately and realistically.

(4) Complete realistic launch-criterion profiles may be obtained by this technique. These launch-criterion profiles are of particularly great importance when vehicles are designed to a 90-percent or 95-percent criterion and when a much higher probability of success is desired for actual launch.

(5) The objectivity of the method results in profiles which provide consistent criteria for various locations and situations and which also provide launch criteria that are consistent with the design criteria. Thus, this method facilitates the designing of vehicles for various missions and various conditions to a single standardized set of wind statistics.

SYMBOLS

a,b	orthogonal components of horizontal wind velocity in a coordinate system which has been rotated through an angle θ from true north
$f( )$	frequency function, or probability density function, of designated variable
$f(;)$	joint frequency function of two designated variables
N	number of observations used in determining a statistical estimate
n	number of standard deviations from mean which include a given probability
u	west-to-east (zonal) component of wind velocity

v south-to-north (meridional) component of wind velocity

Z normalizing transformation of correlation coefficient of normal variables

z height above earth's surface

$\epsilon( )$ error of designated quantity

θ angle of rotation of coordinate system clockwise from true north

ρ correlation coefficient; represents either the estimated value or the unknown population value

σ standard deviation; represents either the estimated value or the unknown population value

Subscripts:

a refers to component of velocity a

b refers to component of velocity b

i refers to value of variable at key or reference height level

j refers to value of variable at height level above or below key level

$j:i$ conditional value of variable at height level z_j contingent upon occurrence of given value of variable at key height level z_i

u refers to component of velocity u

v refers to component of velocity v

Superscripts:

$*$ indicates extreme value

$-$ mean value of variable; represents either the estimated value or the unknown population value

BASIS FOR STATISTICAL MODEL PROFILES

Synthetic Profiles

The usual representation of extreme wind and wind-shear (change of wind with height) conditions for vehicle design purposes is a synthetic wind profile, such as those in references 6 to 9. These profiles are constructed to represent, for some reference level, the most severe wind and wind-shear conditions expected in

some given large percentage of cases, for example, 99 percent. The response of the vehicle to this extreme condition is then determined by a mathematical simulation of vehicle flight through this artificial profile. Inasmuch as this procedure furnishes the extreme loads only in the vicinity of the key or reference level, it is necessary to use profiles having a number of different key levels in order to include all of the critical-flight regions.

A fundamental limitation of synthetic profiles is their inability to simulate the resonant excitation of the fundamental structural modes of the vehicle. Furthermore, short wave-length wind disturbances which produce this excitation of vehicle vibration modes have been filtered out of the radiosonde wind data, which constitute the only presently available sample of wind data large enough to permit statistical treatment. Thus, the small-scale, or gust, component must be treated separately, and the resulting loads must be combined with the loads from the synthetic profile. Methods of treating these small-scale disturbances are outside the scope of the present report; it is merely pointed out that some treatment of these disturbances is a necessary part of the complete solution.

Several synthetic wind profiles which have been used in the past are shown in figure 1. All of these have been used to design vehicles which have been launched at Cape Canaveral, and all are intended to represent a 99-percent probability level. Nevertheless, considerable differences among the various profiles are apparent. Although some of these profiles are military criteria and are intended to represent the most severe wind conditions for the entire United Sates, the greatest differences occur between profiles specifically intended for Cape Canaveral. These differences may be attributed to the limited amount of data available and to the fact that many of the highest winds which actually occur are not measured because the balloons used to measure the wind profiles have been blown beyond the horizon; and even when a balloon is not beyond the horizon, in high-wind situations it is generally at a very low elevation angle, which results in unusually large errors in the measured winds. (See refs. 10 and 11.)

The large differences noted in figure 1 demonstrate the need for consistent, stable estimates of extreme wind conditions. The use of a fitted statistical model of the wind distribution furnishes estimates of extreme conditions which are much more stable than empirical values. It also allows objective construction of the synthetic profiles which provides consistent criteria for various locations and situations.

Statistical Wind Distribution

The form of the statistical wind distribution has been the subject of considerable study; for example, see references 12 to 16. It has been found that the distribution of wind velocity at a given height can be closely approximated by a vector normal (Gaussian) distribution, that is to say, a joint normal distribution of velocity components. Because, in the general case, lines of equal probability form ellipses, this general case is frequently referred to as an elliptical normal distribution. In the special case where the components are uncorrelated and have equal standard deviations, these ellipses reduce to circles, and this special case is called a circular normal distribution. At many locations

the wind-velocity distribution can be closely approximated by a circular normal distribution, but at some locations it is necessary to use the more general elliptical normal form.

It is also found that wind components at different heights are correlated. Since the wind components at the different heights are individually normally distributed and are correlated, their joint distribution may also be treated as a joint normal distribution. This makes it possible to determine conditional or contingent distributions - that is, the distributions of wind components at one altitude contingent upon occurrence of a particular value at the other altitude. These conditional distributions, which can be found by standard statistical techniques described in appendix A, form the basis for the construction of the synthetic wind profiles from the statistical model of the wind distribution.

CONSTRUCTION OF SYNTHETIC PROFILES FROM PARAMETERS OF THE MULTIVARIATE NORMAL DISTRIBUTION

In this section the methods of constructing synthetic profiles from the parameters of multivariate normal distribution are outlined both for design-criterion profiles and for launch-criterion profiles. The mathematical derivations of equations given in this section are given in appendix A. The method of construction given here involves finding the highest value of the wind-velocity component at the key or reference level z_i which will occur within the given probability level, and then finding for each other level z_j above and below the key level the lowest value of the wind-velocity component which will occur within the given probability if this highest value occurs at the key level. For z_j below the key level, this lowest wind component corresponds to the highest positive wind shear between the level z_j and the key level z_i, and for z_j above the key level, this lowest component corresponds to the highest negative wind shear between z_j and z_i; these conditions generally produce the most severe loads. It should be noted that this conditional extreme shear will usually be greater than the extreme of all the shears for the critical altitudes of present-day vehicles and for United States missile ranges, although it is not necessarily greater for all altitudes or for all locations; nor, is it necessarily greater than the extreme of all shears taken without regard to sign. Generally, however, it is a more accurate representation of the extreme loading condition. A derivation and discussion of confidence limits for the statistical-model synthetic profiles is presented in appendix B.

Design-Criterion Profiles

Equations for profile construction.- Profiles which satisfy the conditions just described can be constructed by substituting appropriate values into the following equations:

$$a_i^* = \overline{u_i} \cos\theta - \overline{v_i} \sin\theta + n\sqrt{\sigma_{u_i}^2\cos^2\theta + \sigma_{v_i}^2\sin^2\theta - 2\rho_{u_iv_i}\sigma_{u_i}\sigma_{v_i} \sin\theta \cos\theta} \tag{1}$$

$$b_i^* = \overline{u_i} \sin\theta + \overline{v_i} \cos\theta + n\sqrt{\sigma_{u_i}^2\sin^2\theta + \sigma_{v_i}^2\cos^2\theta + 2\rho_{u_iv_i}\sigma_{u_i}\sigma_{v_i} \sin\theta \cos\theta} \tag{2}$$

$$a_j^* = \overline{u_j}\cos\theta - \overline{v_j}\sin\theta + a_i^*\left(\rho_{u_iu_j}\frac{\sigma_{u_j}}{\sigma_{u_i}}\cos^2\theta + \rho_{v_iv_j}\frac{\sigma_{v_j}}{\sigma_{v_i}}\sin^2\theta\right) - \left(\overline{u_i}\rho_{u_iu_j}\frac{\sigma_{u_j}}{\sigma_{u_i}}\cos\theta - \overline{v_i}\rho_{v_iv_j}\frac{\sigma_{v_j}}{\sigma_{v_i}}\sin\theta\right)$$

$$- n\sqrt{\left(\sigma_{u_j}\sqrt{1-\rho_{u_iu_j}^2}\cos\theta\right)^2 - 2\rho_{u_jv_j}\left(\sigma_{u_j}\sqrt{1-\rho_{u_iu_j}^2}\cos\theta\right)\left(\sigma_{v_j}\sqrt{1-\rho_{v_iv_j}^2}\sin\theta\right) + \left(\sigma_{v_j}\sqrt{1-\rho_{v_iv_j}^2}\sin\theta\right)^2} \tag{3}$$

$$b_j^* = \overline{u_j}\sin\theta + \overline{v_j}\cos\theta + b_i^*\left(\rho_{u_iu_j}\frac{\sigma_{u_j}}{\sigma_{u_i}}\sin^2\theta + \rho_{v_iv_j}\frac{\sigma_{v_j}}{\sigma_{v_i}}\cos^2\theta\right) - \left(\overline{u_i}\rho_{u_iu_j}\frac{\sigma_{u_j}}{\sigma_{u_i}}\sin\theta + \overline{v_i}\rho_{v_iv_j}\frac{\sigma_{v_j}}{\sigma_{v_i}}\cos\theta\right)$$

$$- n\sqrt{\left(\sigma_{u_j}\sqrt{1-\rho_{u_iu_j}^2}\sin\theta\right)^2 + 2\rho_{u_jv_j}\left(\sigma_{u_j}\sqrt{1-\rho_{u_iu_j}^2}\sin\theta\right)\left(\sigma_{v_j}\sqrt{1-\rho_{v_iv_j}^2}\cos\theta\right) + \left(\sigma_{v_j}\sqrt{1-\rho_{v_iv_j}^2}\cos\theta\right)^2} \tag{4}$$

where b^* is the extreme value of the tail wind in the pitch plane of a vehicle launched in direction θ (measured clockwise from true north) and a^* is the extreme value of the left-to-right cross-wind component which will occur within a given probability; $\overline{u_i}$, $\overline{u_j}$, $\overline{v_i}$, and $\overline{v_j}$ are the mean values of the west-to-east and south-to-north components of the wind velocity at levels z_i and z_j, respectively; σ_{u_i}, σ_{u_j}, σ_{v_i}, and σ_{v_j} are the standard deviations of the components u and v at z_i and z_j; and $\rho_{u_iv_i}$, $\rho_{u_jv_j}$, $\rho_{u_iu_j}$, and $\rho_{v_iv_j}$ are the correlation coefficients between the indicated wind components at the indicated heights. Extreme tail-wind components and extreme right-to-left cross-wind components can be found by making a 180° change in the angle θ.

For the west-to-east and south-to-north components, equations (1) to (4) can be reduced to

$$u_j^* = \overline{u_j} + n\sigma_{u_j}\left(\rho_{u_iu_j} - \sqrt{1-\rho_{u_iu_j}^2}\right) \tag{5}$$

and

$$v_j^* = \overline{v_j} + n\sigma_{v_j}\left(\rho_{v_iv_j} - \sqrt{1-\rho_{v_iv_j}^2}\right) \tag{6}$$

where u_i^* and v_i^* are found by setting $u_j = u_i$, $v_j = v_i$, and $\rho_{u_iu_j} = \rho_{v_iv_j} = 1$.

Sources of wind-distribution parameters.- The required parameters of the wind distribution (that is, the mean values, the standard deviations, and the correlations) may be obtained from several sources. A number of tabulations of these parameters have recently been published for several locations of interest (for example, refs. 17 to 21) and others are currently being prepared by various groups. Where required, additional tabulations can be prepared from climatological wind data from standard climatological sources, such as the National Weather Records Center, Asheville, North Carolina, or the World Meteorological Organization, Geneva, Switzerland. When new tabulations are made from standard climatological data, a considerable amount of effort must be devoted to recomputation and serial completion of raw wind data in order to obtain reliable statistical values.

Construction of Launch-Criterion Profiles

Design-criterion profiles based on climatological data specify the most severe wind and wind-shear conditions which will occur within a given probability for all cases in a given season. As the scheduled launch time for a particular vehicle approaches, it is important to know the most severe conditions which may occur at this actual launch time. This is particularly important where the vehicle has been designed to a relatively low-probability wind criterion, such as the 95-percent and even the 90-percent wind criteria used in many current space-vehicle systems. A modification of the technique outlined in the previous section provides launch-criterion profiles for the particular time of scheduled launching.

Launch-criterion profiles based on measured winds.- Wind measurements are usually made as near to launch time as possible. However, because of the time required for measurement, data reduction, analysis, and decision, the final go/no-go decision must always be based on wind measurements made some time in advance of the launch time. Thus, the possible variation in winds between the time of the measurement and the launch time must be accounted for in the launch criterion. Synthetic profiles which take these changes into account can be constructed by substituting appropriate values into equations (1) to (4). The values to be used in the launch-criterion profile based on wind measurements a short time before launch are as follows:

(1) For $\bar{u}_i$, $\bar{v}_i$, $\bar{u}_j$, and $\bar{v}_j$, the measured values of u_i, v_i, u_j, and v_j.

(2) For σ_{u_i}, σ_{v_i}, σ_{u_j}, and σ_{v_j}, the root-mean-square (rms) change of the wind components u_i, v_i, u_j, and v_j over the time interval between measurement and launch.

(3) For $\rho_{u_i v_i}$, $\rho_{u_j v_j}$, $\rho_{u_i u_j}$, and $\rho_{v_i v_j}$ the same climatological values used for the design profiles.

The climatological correlation coefficients may be obtained from the sources listed in the previous sections. A number of measurements of the rms time change are summarized in reference 22, and, of course, new values may be tabulated for particular locations, heights, and seasons needed.

Launch-criterion profiles based on wind forecasts.- For planning and scheduling purposes, it is desirable to know the probability that wind conditions will permit launching well in advance of the scheduled launch time. For periods of time longer than about 3 days, a climatological "forecast" will generally provide the best estimate. A synthetic profile for any given level of probability can be constructed from climatological data in exactly the same way as the design profiles are constructed, except that the parameters chosen will be those appropriate to the season and conditions of the actual launching, which may not be the same as were used in the original vehicle design.

For shorter periods of time, a better estimate can be made by using forecast winds if the standard error (rms error) of the wind forecast is known. Because forecasts of wind velocity are much more accurate than forecasts of wind shear, forecast values are used only for the wind at the key level z_i.

The synthetic profile based on the forecast wind is constructed by making the following substitutions in equations (1) to (4):

$\overline{u_i}, \overline{v_i}$ = Components of forecast wind at height z_i

$\sigma_{u_i} = \sigma_{v_i}$ = Standard error of forecast

and

$$\rho_{u_i v_i} = 0$$

$\overline{u}_j$, $\overline{v}_j$, σ_{u_j}, σ_{v_j}, $\rho_{u_i u_j}$, $\rho_{v_i v_j}$, and $\rho_{u_j v_j}$ are taken from appropriate climatological values.

Application of launch-criterion profiles.- In the section entitled "Construction of Launch-Criterion Profiles," three types of launch-criterion profiles were described. These profiles were based on climatological data, on wind forecasts, and on measured winds. In actual space-vehicle operations they might be employed as follows:

(1) The profiles based on climatological profiles would be used for long-range planning and scheduling and, in fact, for all decisions concerning launchings scheduled more than 3 days in the future.

(2) Profiles based on forecast winds would be used for short-range planning and scheduling - that is, for periods of time from 1 to 3 days.

(3) Profiles based on measured winds would be used for the final go/no-go decision. These winds would be measured just long enough before the scheduled launch time to permit the necessary load computations.

EXAMPLES OF STATISTICAL PROFILES

Figure 2 shows the zonal-component synthetic profiles computed by the procedure described in the previous section for $n = 3$ (approximately 99 percent) for the month of March at the Atlantic Missile Range, along with several other 99-percent design profiles from figure 1. The wind distribution parameters used are taken from reference 21. In this figure the profile has been displaced slightly to make the 11-kilometer peak correspond with the 35,000-foot peak of the other profiles. The month of March is often considered the windiest month at Cape Canaveral, and 11 kilometers is near the most critical level for some vehicles which are of interest. Notice that negative component values are found at the lower altitudes. This is also true of the 95-percent ($n = 2$) profiles, although the 99-percent profile has an algebraically lower value than the 95-percent profile at the lower altitudes. Features such as these are necessarily lost in a profile based on the magnitude of velocity.

Notice also that although the peak velocity is less than the commonly used 300 feet per second, the difference between the highest wind component and the lowest wind component is slightly in excess of 300 feet per second. Thus, it appears that though the statistical model profile is less severe than those presently in use in some respects, it is more severe in other respects.

Corresponding statistical-model profiles for zonal and meridional components are shown in figure 3 for a key level of 10 kilometers. Since the mean wind at the key level of 10 kilometers is negative, the algebraically lowest 99-percent wind has a larger magnitude than the algebraically highest wind. Thus, a negative key-level wind, as illustrated in figure 3(b), will produce the most severe loading, unless the vehicle in question happens to be more critical with respect to winds from the opposite direction.

Except for the negative peaks and the lower magnitudes, the meridional profile is generally similar in character to the profile for the zonal component. Notice that in figure 3(b) the sign of the wind component changes at the upper levels as well as at the lower levels.

Figures 4 and 5 illustrate the changes in the profiles with changing values of the key level. For the meridional profiles in figure 5, both positive and negative extreme values are shown. Only the positive values are shown for the zonal component in figure 4, because the extreme negative values of this component are very small at Cape Canaveral and are not usually of concern for design purposes. Notice that the sharpness of the shear spike varies with each change of key level. This permits a more accurate evaluation of loading at a particular level than a method which simply "slides" a spike of fixed shape up and down for different key levels.

In figures 6 and 7 statistical-model profiles are presented for Santa Maria, California, which is representative of at least a portion of the Pacific Missile Range. The wind-distribution parameters used are taken from reference 21. These profiles apply to the month of February, which has the highest 99-percent level winds at Santa Maria. Several differences between the Santa Maria profiles and the Cape Canaveral profiles are readily apparent. The largest zonal component

values at Santa Maria are lower than those at Cape Canaveral, and the largest values of both the zonal and the meridional components occur at lower altitudes than at Cape Canaveral. Also, at Santa Maria the meridional extreme winds are of nearly the same magnitude as the zonal extreme winds. Of course, other less readily apparent differences might produce quite different effects on the simulated flight of a particular vehicle through the profiles.

CONCLUDING REMARKS

A versatile technique based on the joint normal (Gaussian) distribution of wind components has been presented. This technique makes possible the rapid construction, on a consistent basis, of accurate objective profiles for a wide variety of specific situations, including variations of location, season, launch azimuth, and critical altitude. These synthetic profiles can be constructed for either design criteria or launching criteria. Launch-criterion profiles may be based on climatological data for long-range planning, on wind forecasts for short-range planning, and on measured winds for final decisions.

Langley Research Center,
National Aeronautics and Space Administration,
Langley Station, Hampton, Va., April 15, 1963.

APPENDIX A

DERIVATION OF STATISTICAL-MODEL SYNTHETIC WIND PROFILES

The following derivation is based on the assumption that the joint distribution of wind components at various height levels is a multivariate normal (Gaussian) distribution. The validity of this assumption is discussed in the text of this report. It should be pointed out, however, that even if a better approximation to the actual distribution is found, the present statistical-model synthetic profile can still be used by means of a normalizing transformation - that is, the substitution of a derived, normally distributed variable for the original non-Gaussian variable. The probability density function, or frequency function, of the joint normal distribution of wind components is

$$f(u;v) = \frac{1}{2\pi\sigma_u\sigma_v\sqrt{1 - \rho_{u,v}^2}} \exp\left\{-\frac{1}{2\left(1 - \rho_{u,v}^2\right)}\left[\left(\frac{u - \bar{u}}{\sigma_u}\right)^2 - 2\rho_{u,v}\frac{u - \bar{u}}{\sigma_u}\frac{v - \bar{v}}{\sigma_v} + \left(\frac{v - \bar{v}}{\sigma_v}\right)^2\right]\right\} \tag{A1}$$

Because ellipses are formed by the curves of $f(u;v) = \text{Constant}$, this distribution is referred to as an elliptical normal distribution. If $\sigma_u = \sigma_v$ and $\rho_{u,v} = 0$, curves of $f(u;v) = \text{Constant}$ become circles; this special case called a circular normal distribution. The wind-velocity distribution at many locations can be approximated closely by the circular normal, but for greater generality, the elliptical form will be considered in the following development. It should be noted that if the distribution of wind velocity follows the vector normal distribution given by equation (A1), then the magnitude of the velocity vector, or wind speed, will not be normally distributed.

In order to specify the statistics of the vertical wind profile, it is necessary to describe the relationship between winds at various levels as well as the distribution at each level. These relationships are described by interlevel correlation coefficients. A complete description requires not only the correlations between parallel components at different levels but also the correlations between the perpendicular components at different levels. The latter, however, are difficult to compute accurately and contribute relatively little additional information, so they are usually neglected. They will also be neglected in the following development.

The joint distribution of parallel components at two different height levels z_i and z_j is given by

$$f(u_i;u_j) = \frac{1}{2\pi\sigma_{u_i}\sigma_{u_j}\sqrt{1 - \rho_{u_iu_j}^2}} \exp\left\{-\frac{1}{2\left(1 - \rho_{u_iu_j}^2\right)}\left[\left(\frac{u_i - \overline{u_i}}{\sigma_{u_i}}\right)^2\right.\right.$$

$$\left.\left. - 2\rho_{u_iu_j}\frac{u_i - \overline{u_i}}{\sigma_{u_i}}\frac{u_j - \overline{u_j}}{\sigma_{u_j}} + \left(\frac{u_j - \overline{u_j}}{\sigma_{u_j}}\right)^2\right]\right\} \tag{A2}$$

and

$$f(v_i;v_j) = \frac{1}{2\pi\sigma_{v_i}\sigma_{v_j}\sqrt{1 - \rho_{v_iv_j}^2}} \exp\left\{-\frac{1}{2\left(1 - \rho_{v_jv_j}^2\right)}\left[\left(\frac{v_i - \overline{v_i}}{\sigma_{v_i}}\right)^2\right.\right.$$

$$\left.\left. - 2\rho_{v_iv_j}\frac{v_i - \overline{v_i}}{\sigma_{v_i}}\frac{v_j - \overline{v_j}}{\sigma_{v_j}} + \left(\frac{v_j - \overline{v_j}}{\sigma_{v_j}}\right)^2\right]\right\} \tag{A3}$$

Thus, if the interlevel cross-component correlations $\rho_{u_iv_j}$ are neglected, the parameters needed to describe the statistical characteristics of the wind profile are the values of $\overline{u}$, $\overline{v}$, σ_u, and σ_v at each height level and the values of $\rho_{u_iu_j}$ and $\rho_{v_iv_j}$ for all combinations of height levels.

Zonal and Meridional Components

In this section a method of constructing synthetic profiles from the parameters of the multivariate normal distribution is developed. Each profile so constructed represents a particular component of wind. Profiles are developed for meridional and zonal components. In the following section profiles for intermediate components will be formed from combinations of these profiles and the intralevel correlation coefficients $\rho_{u_iv_i}$.

In the present method, the construction of the profile is, as usual, begun with the estimate of an extreme value of the wind at some key level z_i. (This key level may correspond to a critical region in the trajectory of a particular vehicle, such as the transonic region or the region of maximum dynamic pressure, or profiles may be constructed for several key levels in the region of high winds.) However, where the usual procedure has been to estimate an extreme value for the total wind speed, in the present method the extreme value of a particular component is used. The frequency functions of the zonal and meridional components are given by the marginal frequency functions of the joint frequency function given by equation (A1). It is shown in textbooks of mathematical statistics

(for example, ref. 23) that these marginal frequency functions are

$$f(u_i) = \frac{1}{\sqrt{2\pi}\sigma_{u_i}} \exp\left[-\frac{1}{2}\left(\frac{u_i - \overline{u_i}}{\sigma_{u_i}}\right)^2\right] \tag{A4}$$

and

$$f(v_i) = \frac{1}{\sqrt{2\pi}\sigma_{v_i}} \exp\left[-\frac{1}{2}\left(\frac{v_i - \overline{v_i}}{\sigma_{v_i}}\right)^2\right] \tag{A5}$$

which are univariate normal distributions with means $\overline{u_i}$ and $\overline{v_i}$ and with standard deviations σ_{u_i} and σ_{v_i}, respectively. Thus, the desired extreme values are found by

$$u_i^* = \overline{u_i} + n\sigma_{u_i} \tag{A6}$$

and

$$v_i^* = \overline{v_i} + n\sigma_{v_i} \tag{A7}$$

where n is the number of standard deviations required to include the desired probability of occurrence; for example, for a 95-percent probability, $n \approx 2$, and for 99 percent, $n \approx 3$.

Wind component values for the additional levels z_j are determined by finding the value which gives the extreme shear between the level z_j and the key level z_i which will occur together with the extreme wind component value at z_i, for example, the lowest value of u_j which will occur 99 percent of the time if the 99-percent highest value of u_i occurs. Inasmuch as high shears are generally associated with high wind velocity, this value will usually be larger than the 99-percent value for all shears in this layer.

Finding this value for z_j requires a knowledge of the contingent or conditional distribution of the velocity component at z_j given a particular velocity component at z_i. It is shown in statistics texts that the conditional distribution is given by

$$f\left(u_{j:i}\right) = \frac{1}{\sqrt{2\pi}\sigma_{u_j}\sqrt{1 - \rho_{u_i u_j}^2}} \exp\left\{-\frac{1}{2}\left[\frac{u_{j:i} - \overline{u_j} - \rho_{u_i u_j}\frac{\sigma_{u_j}}{\sigma_{u_i}}\left(u_i - \overline{u_i}\right)}{\sigma_{u_j}\sqrt{1 - \rho_{u_i u_j}^2}}\right]^2\right\} \tag{A8}$$

and

$$f\left(v_{j:i}\right) = \frac{1}{\sqrt{2\pi}\sigma_{v_j}\sqrt{1 - \rho_{v_i v_j}^2}} \exp\left\{-\frac{1}{2}\left[\frac{v_{j:i} - \overline{v_j} - \rho_{v_i v_j}\frac{\sigma_{v_j}}{\sigma_{v_i}}\left(v_i - \overline{v_i}\right)}{\sigma_{v_j}\sqrt{1 - \rho_{v_i v_j}^2}}\right]^2\right\} \tag{A9}$$

Equations (A8) and (A9) have the form of normal distributions whose means are

$$\overline{u_{j:i}} = \overline{u_j} + \rho_{u_i u_j}\frac{\sigma_{u_j}}{\sigma_{u_i}}\left(u_i - \overline{u_i}\right) \tag{A10}$$

and

$$\overline{v_{j:i}} = \overline{v_j} + \rho_{v_i v_j}\frac{\sigma_{v_j}}{\sigma_{v_i}}\left(v_i - \overline{v_i}\right) \tag{A11}$$

and whose standard deviations are

$$\sigma_{u_{j:i}} = \sigma_{u_j}\sqrt{1 - \rho_{u_i u_j}^2} \tag{A12}$$

and

$$\sigma_{v_{j:i}} = \sigma_{v_j}\sqrt{1 - \rho_{v_i v_j}^2} \tag{A13}$$

Thus, the lower extreme values of $u_{j:i}$ and $v_{j:i}$ (which correspond to the upper extreme values of shear between z_j and z_i) are given by

$$u_j^* = u_{j:i}^* = \overline{u_{j:i}} - n\sigma_{u_{j:i}} \tag{A14}$$

and

$$v_j^* = v_{j:i}^* = \overline{v_{j:i}} - n\sigma_{j:i} \tag{A15}$$

and substituting from equations (A10) to (A13) yields

$$u_j^* = \overline{u_j} + \rho_{u_i u_j} \frac{\sigma_{u_j}}{\sigma_{u_i}}\left(u_i^* - \overline{u_i}\right) - n\sigma_{u_j}\sqrt{1 - \rho_{u_i u_j}^2} \tag{A16}$$

and

$$v_j^* = \overline{v_j} + \rho_{v_i v_j} \frac{\sigma_{v_j}}{\sigma_{v_i}}\left(v_i^* - \overline{v_i}\right) - n\sigma_{v_j}\sqrt{1 - \rho_{v_i v_j}^2} \tag{A17}$$

Inasmuch as the u_i^* and v_i^* are the extreme values u_i and v_i, substituting equations (A6) and (A7) in equations (A16) and (A17), respectively, yields

$$u_j^* = \overline{u_j} + n\sigma_{u_j}\left(\rho_{u_i u_j} - \sqrt{1 - \rho_{u_i u_j}^2}\right) \tag{A18}$$

and

$$v_j^* = \overline{v_j} + n\sigma_{v_j}\left(\rho_{v_i v_j} - \sqrt{1 - \rho_{v_i v_j}^2}\right) \tag{A19}$$

Equations (A18) and (A19) provide a means for rapidly constructing the profiles for the zonal and meridional components from the parameters of the multivariate normal distribution. Note that if $i = j$, then $\rho_{u_i u_j} = \rho_{v_i v_j} = 1$, and equations (A18) and (A19) reduce to equations (A6) and (A7). Also notice that equations (A6), (A7), and (A16) to (A19) yield the largest algebraic values of key-level wind and the lowest algebraic values of wind at other levels; thus, these equations yield the highest algebraic values of wind shear which will occur within the desired probability level. This value will correspond to the extreme magnitude of wind and shear if, and only if, the sign of $\overline{u_i}$ or $\overline{v_i}$ is positive. If extreme values of the magnitudes are desired, as will very often be the case, they can be found from equations (A18) and (A19) by assigning n the same sign as $\overline{u_i}$ or $\overline{v_i}$.

Intermediate Components

Usually the wind components which are of interest will be the components parallel with and perpendicular to the line of flight of the vehicle. Since these are not necessarily north-south or east-west components, a method for constructing synthetic profiles for intermediate components is also needed.

Consider a right-hand orthogonal system with velocity components a and b where the b-axis is directed at angle θ clockwise from true north. For example,

if θ is the down-range direction, the component b represents a tail-wind component and the component a represents a cross wind from left to right. These components can be expressed in terms of u and v by

$$a = u \cos \theta - v \sin \theta \tag{A20}$$

and

$$b = u \sin \theta + v \cos \theta \tag{A21}$$

These tranformation equations could, of course, be applied to the raw wind data and new wind distribution parameters computed. However, it seems more desirable to develop profiles directly from the distribution parameters for the standard zonal and meridional components, so that profiles for any launch azimuth can be quickly constructed from a compact set of wind statistics.

A derivation of the mean and standard deviation of intermediate-axis components is given in reference 16. In the notation and sign convention of the present report the means are

$$\overline{a} = \overline{u} \cos \theta - \overline{v} \sin \theta \tag{A22}$$

and

$$\overline{b} = \overline{u} \sin \theta + \overline{v} \cos \theta \tag{A23}$$

and the standard deviations are

$$\sigma_a = \sqrt{(\sigma_u \cos \theta)^2 - 2\rho_{u,v}\sigma_u\sigma_v \cos \theta \sin \theta + (\sigma_v \sin \theta)^2} \tag{A24}$$

and

$$\sigma_b = \sqrt{(\sigma_u \sin \theta)^2 - 2\rho_{u,v}\sigma_u\sigma_v \sin \theta \cos \theta + (\sigma_v \cos \theta)^2} \tag{A25}$$

For the key altitude level z_i the extreme values are

$$a_i^* = \overline{a_i} + n\sigma_{a_i} \tag{A26}$$

and

$$b_i^* = \overline{b_i} + n\sigma_{b_i} \tag{A27}$$

and are found by simply substituting values from equations (A22) to (A25) into equations (A26) and (A27):

$$a_i^* = \overline{u_i} \cos\theta - \overline{v_i} \sin\theta + n\sqrt{\sigma_{u_i}^2 \cos^2\theta + \sigma_{v_i}^2 \sin^2\theta - 2\rho_{u_i v_i}\sigma_{u_i}\sigma_{v_i} \sin\theta \cos\theta} \tag{A28}$$

$$b_i^* = \overline{u_i} \sin\theta + \overline{v_i} \cos\theta + n\sqrt{\sigma_{u_i}^2 \sin^2\theta + \sigma_{v_i}^2 \cos^2\theta + 2\rho_{u_i v_i}\sigma_{u_i}\sigma_{v_i} \sin\theta \cos\theta} \tag{A29}$$

For the additional levels z_j the extreme value a_j^* is found as follows:

(1) a_i^* is projected onto the u- and v-axes.

(2) The conditional means and conditional standard deviations of u_j and v_j, given these projected values of u_i and v_i, are found as before.

(3) These values, along with the cross-component correlation $\rho_{u_j v_j}$ at height z_j, are substituted into equations (A22) and (A24) to find the conditional mean and conditional standard deviation of a_j.

(4) The extreme value a_j^* is found from

$$a_j^* = \overline{a_{j:i}} - n\sigma_{a_{j:i}} \tag{A30}$$

The result of this procedure is

$$a_j^* = \overline{u_j} \cos\theta - \overline{v_j} \sin\theta + a_i^*\left(\rho_{u_i u_j}\frac{\sigma_{u_j}}{\sigma_{u_i}}\cos^2\theta + \rho_{v_i v_j}\frac{\sigma_{v_j}}{\sigma_{v_i}}\sin^2\theta\right) - \left(\overline{u_i}\rho_{u_i u_j}\frac{\sigma_{u_j}}{\sigma_{u_i}}\cos\theta - \overline{v_i}\rho_{v_i v_j}\frac{\sigma_{v_j}}{\sigma_{v_i}}\sin\theta\right)$$
$$- n\sqrt{\left(\sigma_{u_j}\sqrt{1-\rho_{u_i u_j}^2}\cos\theta\right)^2 - 2\rho_{u_j v_j}\left(\sigma_{u_j}\sqrt{1-\rho_{u_i u_j}^2}\cos\theta\right)\left(\sigma_{v_j}\sqrt{1-\rho_{v_i v_j}^2}\sin\theta\right) + \left(\sigma_{v_j}\sqrt{1-\rho_{v_i v_j}^2}\sin\theta\right)^2} \tag{A31}$$

where the a_i^* is given by equation (A28).

Following this same procedure for the component b gives

$$b_j^* = \overline{u_j} \sin\theta + \overline{v_j} \cos\theta + b_i^*\left(\rho_{u_i u_j}\frac{\sigma_{u_j}}{\sigma_{u_i}}\sin^2\theta + \rho_{v_i v_j}\frac{\sigma_{v_j}}{\sigma_{v_i}}\cos^2\theta\right) - \left(\overline{u_i}\rho_{u_i u_j}\frac{\sigma_{u_j}}{\sigma_{u_i}}\sin\theta + \overline{v_i}\rho_{v_i v_j}\frac{\sigma_{v_j}}{\sigma_{v_i}}\cos\theta\right)$$
$$- n\sqrt{\left(\sigma_{u_j}\sqrt{1-\rho_{u_i u_j}^2}\sin\theta\right)^2 + 2\rho_{u_j v_j}\left(\sigma_{u_j}\sqrt{1-\rho_{u_i u_j}^2}\sin\theta\right)\left(\sigma_{v_j}\sqrt{1-\rho_{v_i v_j}^2}\cos\theta\right) + \left(\sigma_{v_j}\sqrt{1-\rho_{v_i v_j}^2}\cos\theta\right)^2} \tag{A32}$$

where b_i^* is given by equation (A29).

As was the case with the zonal and meridional components, these equations yield the extreme algebraic values. These values correspond to the extreme tail-wind and left-to-right cross-wind components. Head-wind and right-to-left cross-wind components can be found by a 180° change in θ.

APPENDIX B

CONFIDENCE LIMITS FOR SYNTHETIC WIND PROFILES

Whenever a statistical estimate is made it is of interest to know the range of variability of the estimate. From equation (5) in the text it can be seen that errors of estimate of the extreme values u_j may originate in the estimation of $\overline{u_j}$, σ_{v_j}, and $\rho_{i,j}$. For the purpose of determining confidence limits it will be assumed that (1) the distribution of the estimates of $\overline{u_j}$ and σ_{u_j} can be adequately approximated by normal distributions, (2) $\rho_{i,j}$ can be normalized by the usual transformation (see ref. 23),

$$\rho = \tanh Z \tag{B1}$$

(3) errors of estimate of $\overline{u_j}$, σ_{v_j}, and $\rho_{i,j}$ are independent, and (4) the total error of estimate is normally distributed with zero mean. Thus, the confidence limits for u_j will be given by $u_j \pm n\sigma_{u_j}$. Under the transformation of equation (B1), equation (5) becomes

$$u_j^* = \overline{u_j} + n\sigma_{u_j}\left(\tanh Z_{i,j} - \operatorname{sech} Z_{i,j}\right) \tag{B2}$$

and the error of estimate is

$$\epsilon\left(u_j^*\right) = \epsilon\left(\overline{u_j}\right) + n\sigma_{u_j}\left(\operatorname{sech}^2 Z_{i,j} + \tanh Z_{i,j} \operatorname{sech} Z_{i,j}\right)\epsilon\left(Z_{i,j}\right) + n(\tanh Z - \operatorname{sech} Z)\epsilon\left(\sigma_{u_j}\right) \tag{B3}$$

Again, the inverse transformation of equation (B1) yields

$$\epsilon\left(u_j^*\right) = \epsilon\left(\overline{u_j}\right) + n\sigma_{u_j}\left(1 - \rho^2 + \rho\sqrt{1 - \rho^2}\right)\epsilon\left(Z_{i,j}\right) + n\left(\rho - \sqrt{1 - \rho^2}\right)\epsilon\left(\sigma_{u_j}\right) \tag{B4}$$

and the variance of $\sigma_{u_j}^*$ is

$$\left(\sigma_{u_j}{}^*\right)^2 = \overline{\epsilon\left(u_j{}^*\right)^2} = \sigma_{\overline{u_j}}{}^2 + n^2\sigma_{u_j}{}^2\left(1 - \rho^2 + \rho\sqrt{1 - \rho^2}\right)^2\sigma_{Z_{i,j}}{}^2$$

$$+ n^2\left(\rho - \sqrt{1 - \rho^2}\right)^2\sigma_{\sigma_{u_j}}{}^2 \qquad \text{(B5)}$$

Under the previously listed assumption, the standard deviation of $\overline{u_j}$ is

$$\sigma_{\overline{u_j}} = \frac{\sigma_{u_j}}{\sqrt{N}} \qquad \text{(B6)}$$

The standard deviation of $Z_{i,j}$ is

$$\sigma_{Z_{i,j}} = \frac{1}{\sqrt{N - 3}} \approx \frac{1}{\sqrt{N}} \qquad \text{(B7)}$$

and the standard deviation of σ_{v_j} is

$$\sigma_{\sigma_{v_j}} = \frac{\sigma_{v_j}}{\sqrt{2N}} \qquad \text{(B8)}$$

and substituting equations (B6), (B7), and (B8) into equation (B5) gives the standard deviation of $u_j{}^*$:

$$\sigma_{u_j}{}^* = \frac{\sigma_{u_j}}{\sqrt{N}}\sqrt{1 + n^2\left(\frac{3}{2} + \rho_{u_iu_j}\sqrt{1 - \rho_{u_iu_j}{}^2} - \rho_{u_iu_j}{}^2 - 2\rho_{u_iu_j}{}^3\sqrt{1 - \rho_{u_iu_j}{}^2}\right)} \qquad \text{(B9)}$$

Similarly, the standard deviation of $v_j{}^*$ is given by

$$\sigma_{v_j}{}^* = \frac{\sigma_{v_j}}{\sqrt{N}}\sqrt{1 + n^2\left(\frac{3}{2} + \rho_{v_iv_j}\sqrt{1 - \rho_{v_iv_j}{}^2} - \rho_{v_iv_j}{}^2 - 2\rho_{v_iv_j}{}^3\sqrt{1 - \rho_{v_iv_j}{}^2}\right)} \qquad \text{(B10)}$$

Equations (B9) and (B10) allow the computation of confidence limits for any desired degree of confidence for the north-south and east-west component profiles. The derivation of the standard deviations of the intermediate components

is more complicated; however, the values will generally be on the order of those for the meridional and zonal components.

In figure 8(a) the 99-percent profile for the 10-kilometer key level for the month of March at Cape Canaveral is shown again, together with the upper and lower confidence limits for the actual profile computed by equation (B9).

It would be of interest to compare these confidence limits with confidence limits for empirically constructed profiles which make no assumption concerning the form of the distribution. However, it is not possible to determine the upper confidence limit for such a profile, even for the key-level value, because the largest value of a sample of 660 observations is required (ref. 24) and the available sample contains only 385 observations. This illustrates the difficulty of making precise, stable estimates concerning low-probability occurrences from the amount of wind data available unless a model distribution is used.

Because the variable under consideration is serially correlated, the true confidence bands are actually somewhat wider than those shown in figure 8. (See ref. 18.) The serial correlation coefficients for Cape Canaveral were not available; however, serial correlations for other Florida stations taken from reference 22 indicate that the increase might be between 25 percent and 75 percent. On the other hand, it should be noted that if the distribution parameters were recomputed using all the additional Cape Canaveral wind data which have been acquired up to the present time, the value of N would be about doubled, bringing about a 30-percent decrease in the width of the confidence bands. Thus, the confidence limits shown here and in the following figures represent a realistic estimate of the approximate accuracy which can be achieved by the statistical-model technique, even when the effects of serial correlation are considered.

Figure 8(b) shows the meridional corresponding component 99-percent profile with 99-percent confidence limits, and figures 9(a) and (b) show, respectively, the zonal and meridional component 95-percent profiles each with 95-percent confidence limits. Comparison of the figures shows that the confidence bands for the two components are roughly equal at all altitudes. The increased width of the confidence bands at the higher altitudes is largely a result of decreased sample sizes at these altitudes. As might be expected, the 95-percent confidence bands about the 95-percent profiles are considerably narrower than the 99-percent confidence bands about the 99-percent curves.

REFERENCES

1. Henry, Robert M., Brandon, George W., Tolefson, Harold B., and Lanford, Wade E.: The Smoke-Trail Method for Obtaining Detailed Measurements of the Vertical Wind Profile for Application to Missile-Dynamic-Response Problems. NASA TN D-976, 1961.

2. Reisig, Gerhard: Resumé of Missile Measured Winds at Cape Canaveral, Florida. Rep. No. Da-TR-3-59, Dev. Operations Div., Army Ballistic Missile Agency (Redstone Arsenal, Ala.), Jan. 22, 1959.

3. Trembath, N. W.: Control System Design Wind Criterion. GM-TM-0165-00258, Space Tech. Labs., the Ramo-Wooldridge Corp., June 30, 1958.

4. Bieber, R. E.: Missile Structural Loads by Nonstationary Statistical Methods. Jour. Aerospace Sci., vol. 28, no. 4, April 1961, pp. 284-294.

5. Mazzola, Luciano L.: Design Criteria for Wind Induced Flight Loads on Large Boosted Vehicles. [Preprint] 2408-62, American Rocket Soc., Apr. 1962.

6. Sissenwine, Norman: Windspeed Profile, Wind Shear, and Gusts for Design of Guidance Systems for Vertical Rising Air Vehicles. Air Force Surveys in Geophysics No. 57 (AFCRC-TN-54-22), Air Force Cambridge Res. Center, Nov. 1954.

7. Sissenwine, Norman: Development of Missile Design Wind Profiles for Patrick AFB. Air Force Surveys in Geophysics No. 96 (AFCRC-TN-58-216, ASTIA Doc. No. AD.146870), Air Force Cambridge Res. Center, Mar. 1958.

8. Williams, J. J., and Bergst, G. L., Jr.: Design Wind Criteria for Air Force Missile Test Center. LMSD-2933, Lockheed Aircraft Corp., Apr. 30, 1958.

9. Scoggins, James R., and Vaughan, William W.: Cape Canaveral Wind and Shear Data (1 Thru 80 km) for Use in Vehicle Design and Performance Studies. NASA TN D-1274, 1962.

10. Reiter, Elmar R.: The Layer of Maximum Wind. Jour. Meteorology, vol. 15, no. 1, Feb. 1958, pp. 27-43.

11. Tolefson, H. B.: An Investigation of Vertical-Wind-Shear Intensities From Balloon Soundings for Application to Airplane- and Missile-Response Problems. NACA TN 3732, 1956.

12. Brooks, C. E. P., Durst, C. S., Carruthers, H., Dewar, D., and Sawyer, J. S.: Upper Winds Over the World. Geophys. Mem. No. 85 (vol. X, no. 5), British Meteorological Office, 1950.

13. Crutcher, Harold L.: On the Standard Vector-Deviation Wind Rose. Jour. Meteorology, vol. 14, no. 1, Feb. 1957, pp. 28-33.

14. Crutcher, Harold L.: Meridional Cross-Sections - Upper Winds Over the Northern Hemisphere. Tech. Paper No. 41, Weather Bur., U.S. Dept. Commerce, June 1961.

15. Henry, T. J. G.: Maps of Upper Winds Over Canada. Meteorological Div., Dept. of Transport (Canada), 1957.

16. Weaver, William L., Swanson, Andrew G., and Spurling, John F.: Statistical Wind Distribution Data for Use at NASA Wallops Station. NASA TN D-1249, 1962.

17. Court, Arnold: Vertical Correlations of Wind Components. AFCRC-TN-57-292 (ASTIA Doc. No. 117182), Geophys. Res. Directorate, Air Force Cambridge Res. Center, Mar. 29, 1957.

18. Charles, B. N.: Empirical Models of Interlevel Correlation of Winds. Jour. Meteorology, vol. 16, no. 5, Oct. 1959, pp. 581-585.

19. Charles, B. N.: The U.S. Weather Bureau-Sandia Corporation Co-operative Project in Climatology - Final Report: Upper-Wind Statistics from USWB-FCDA Data. SCTM-302-57-(51) (Contract AT(29-1)-789), Sandia Corp. (Albuquerque, N. Mex.), Dec. 9, 1957.

20. Kochanski, Adam: Models of Vertical Correlations of the Wind. Jour. Meteorology, vol. 18, no. 2, Apr. 1961, pp. 151-159.

21. Vaughan, William W.: Interlevel and Intralevel Correlations of Wind Components for Six Geographical Locations. NASA TN D-561, 1960.

22. Ellsaesser, Hugh W.: Wind Variability. AWS TR 105-2 U.S. Air Force, Mar. 1960.

23. Hoel, Paul G.: Introduction to Mathematical Statistics. Second ed., John Wiley & Sons, Inc., c.1954.

24. Wilks, S. S.: Determination of Sample Sizes for Setting Tolerance Limits. Annals of Mathematical Statistics, vol. 12, 1941, pp. 91-96.

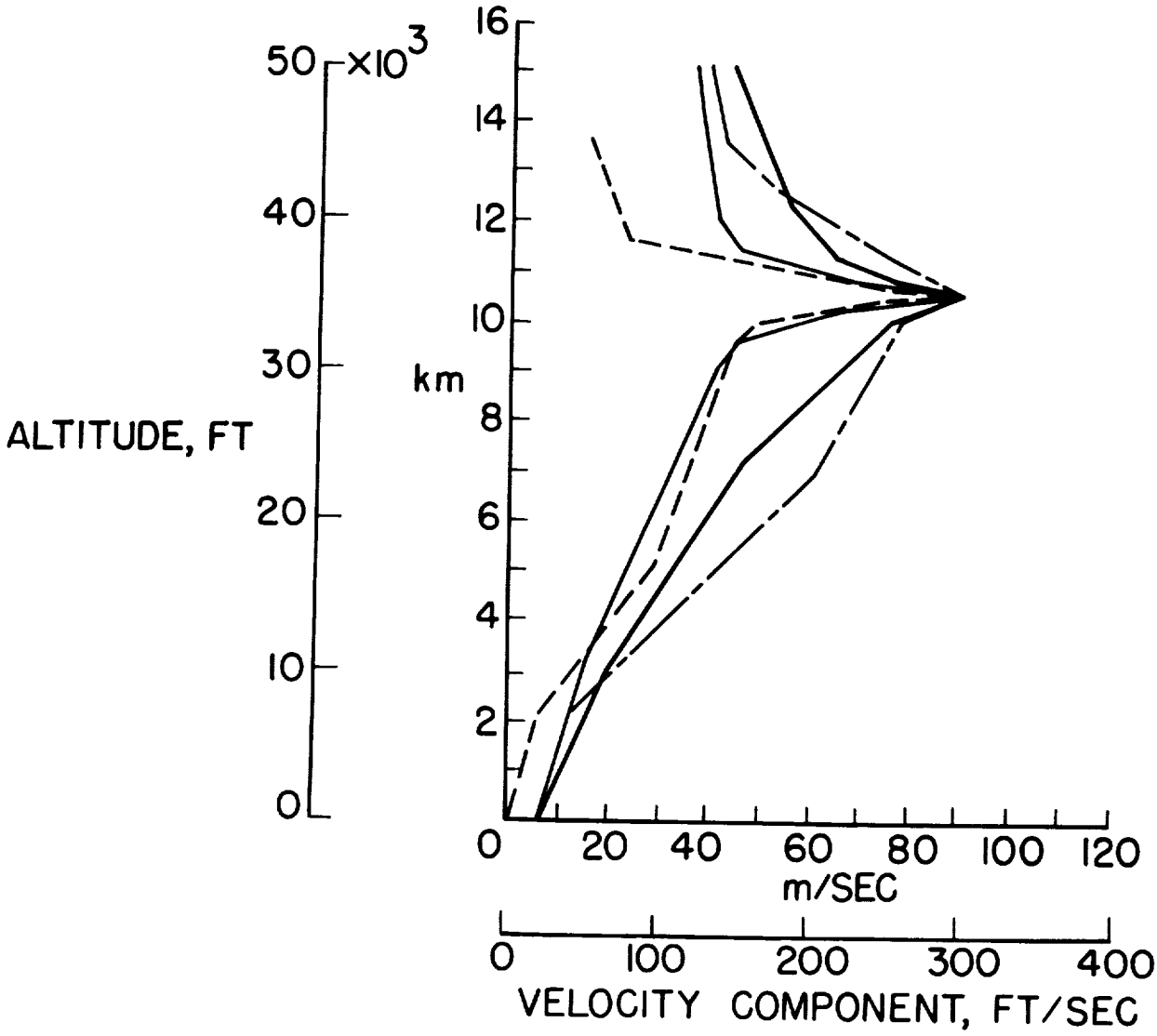

Figure 1.- Comparison of several 99-percent design wind profiles.

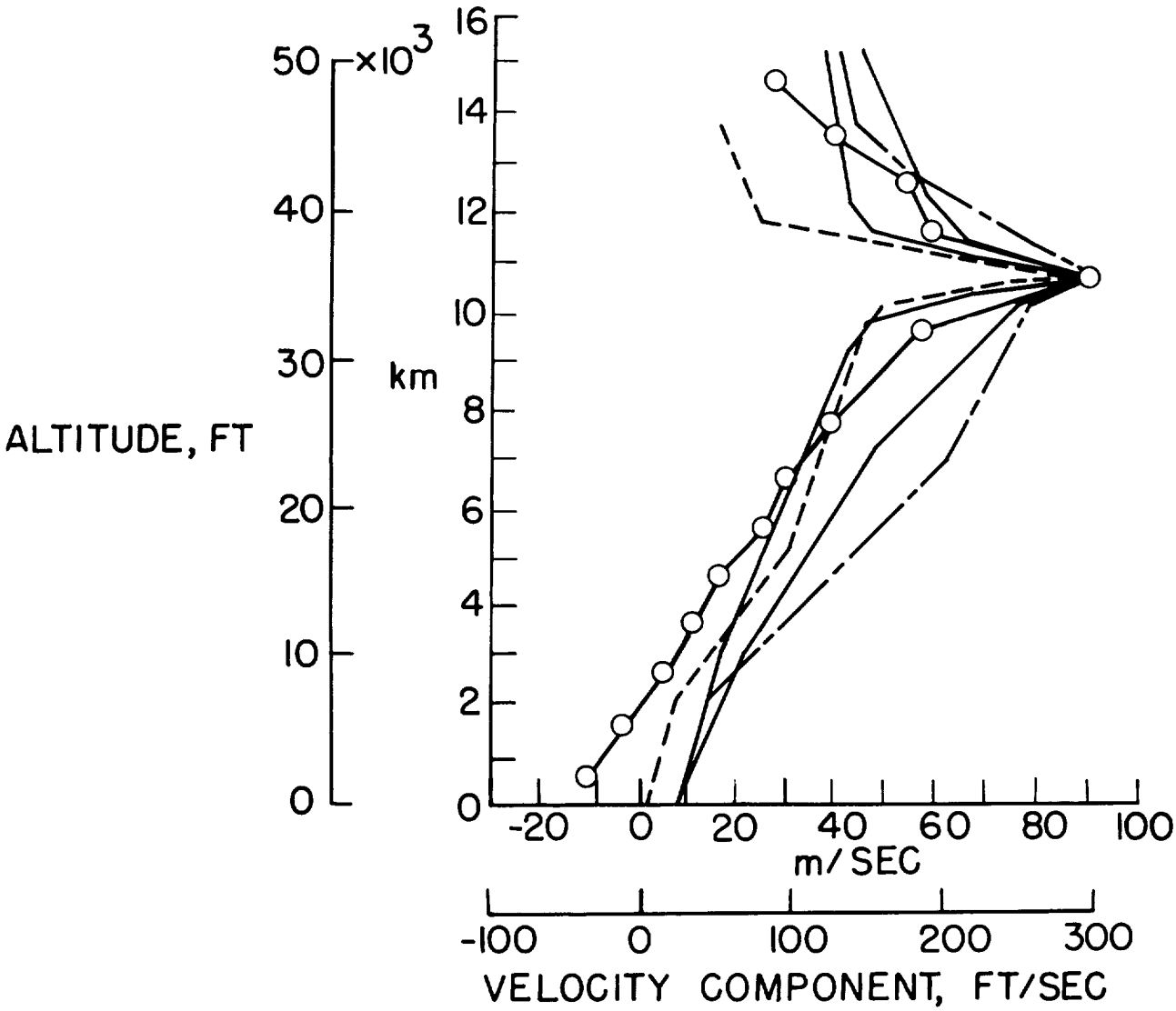

Figure 2.- Comparison of west-to-east—component statistical-model profile and other profiles.

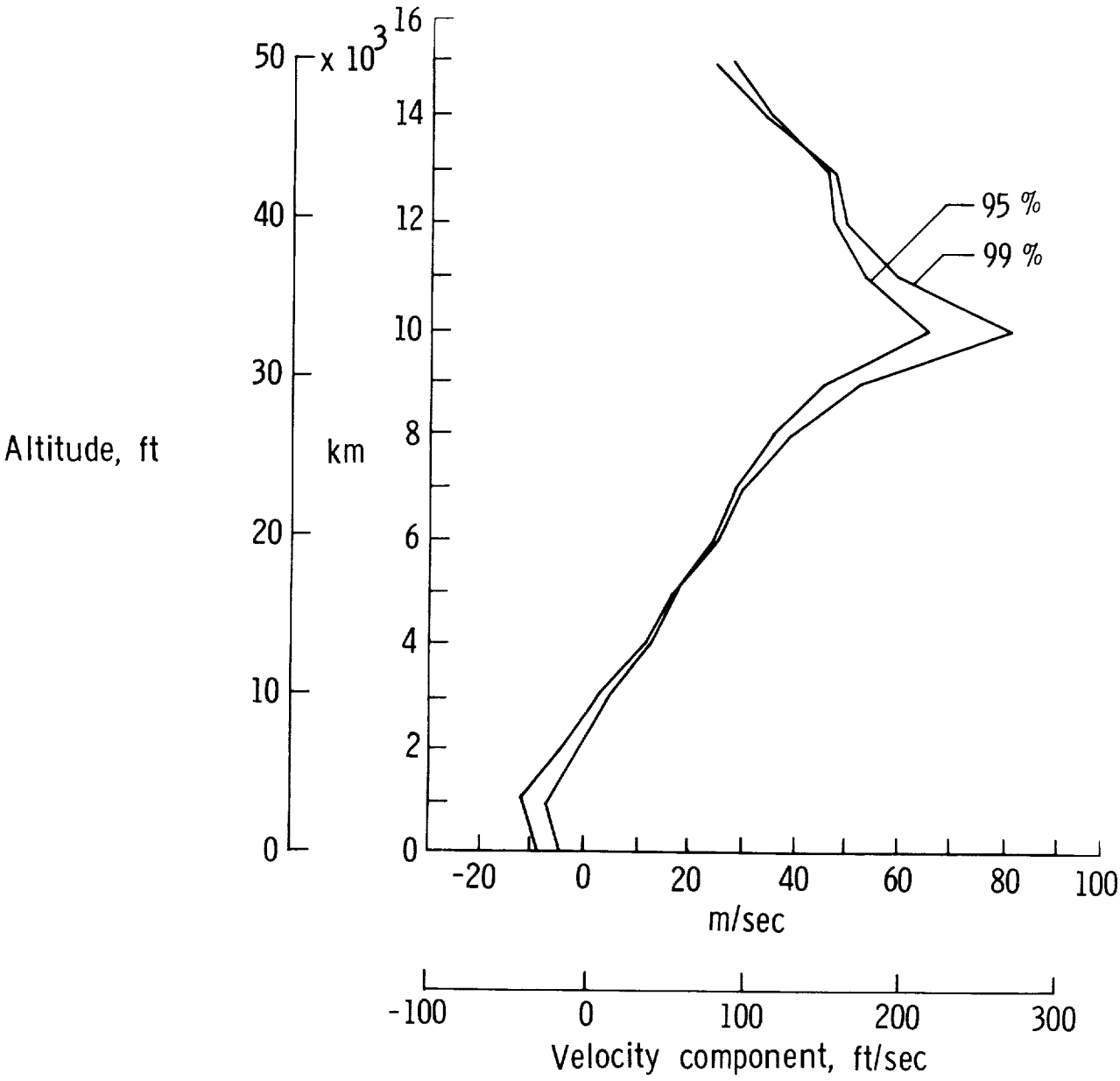

(a) Zonal component.

Figure 3.- Statistical-model profiles for month of March at Cape Canaveral for key level of 10 kilometers.

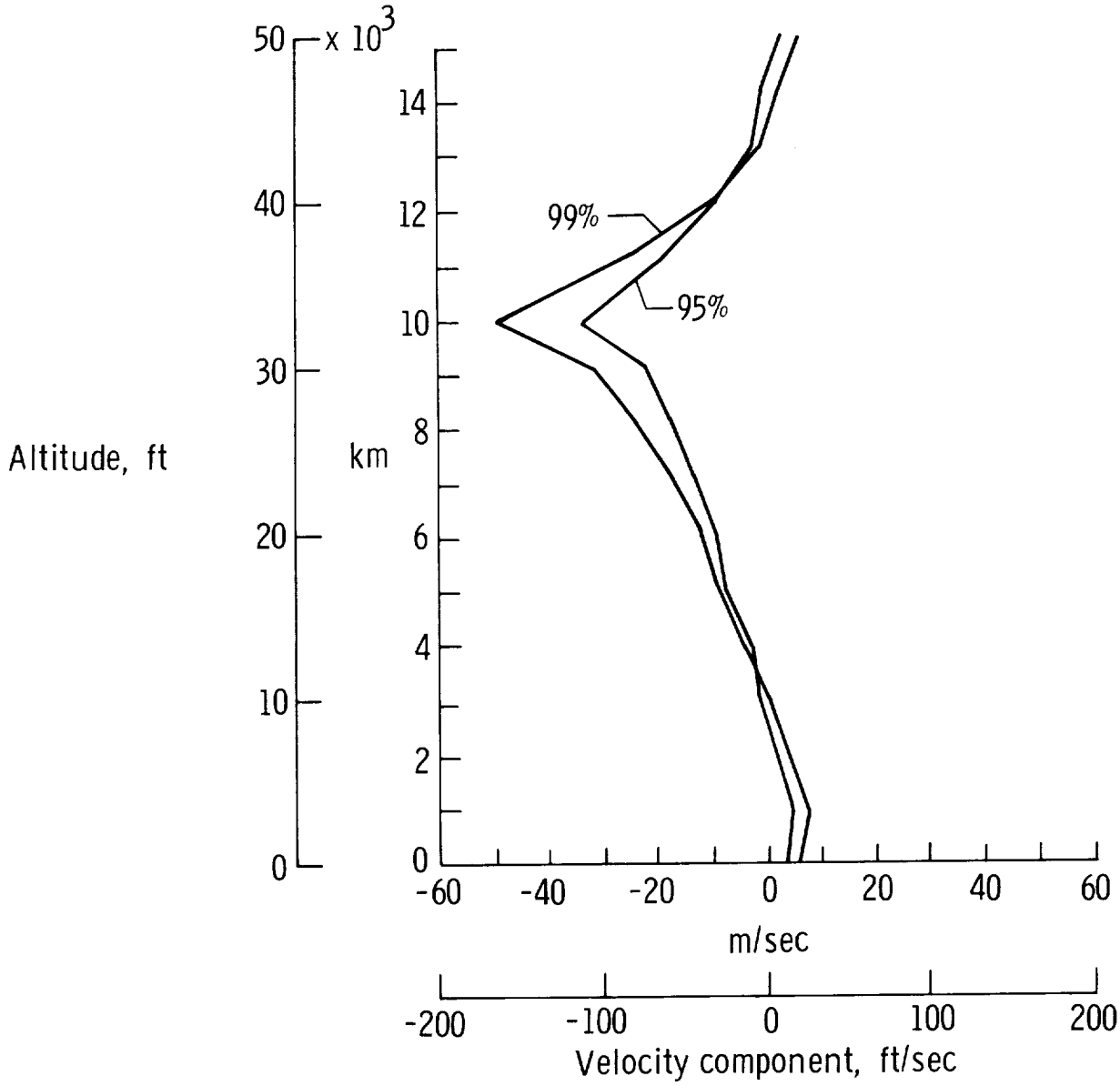

(b) Meridional component.

Figure 3.- Concluded.

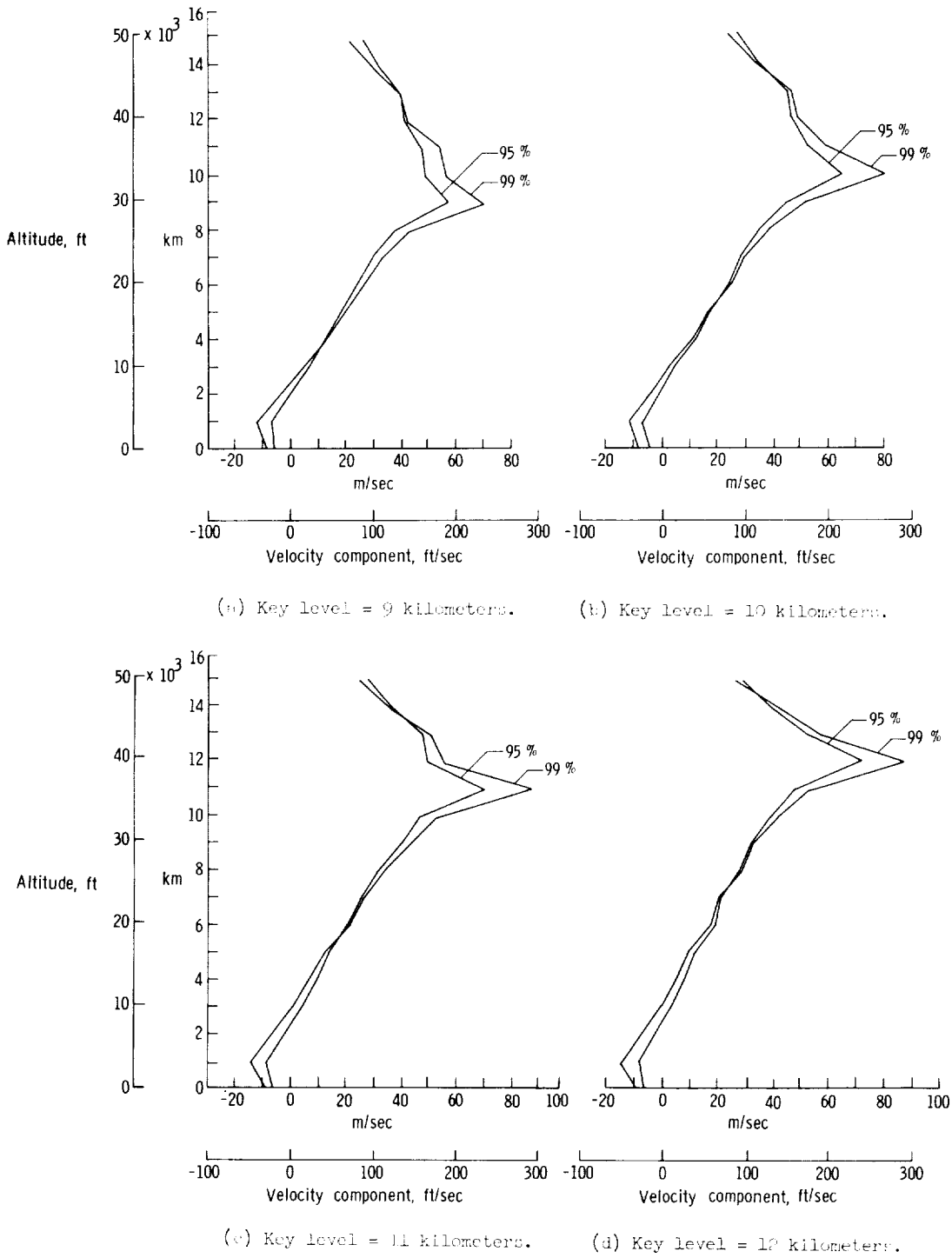

(a) Key level = 9 kilometers. (b) Key level = 10 kilometers.

(c) Key level = 11 kilometers. (d) Key level = 12 kilometers.

Figure 4.- Zonal-component model profiles for month of March at Cape Canaveral for several key levels.

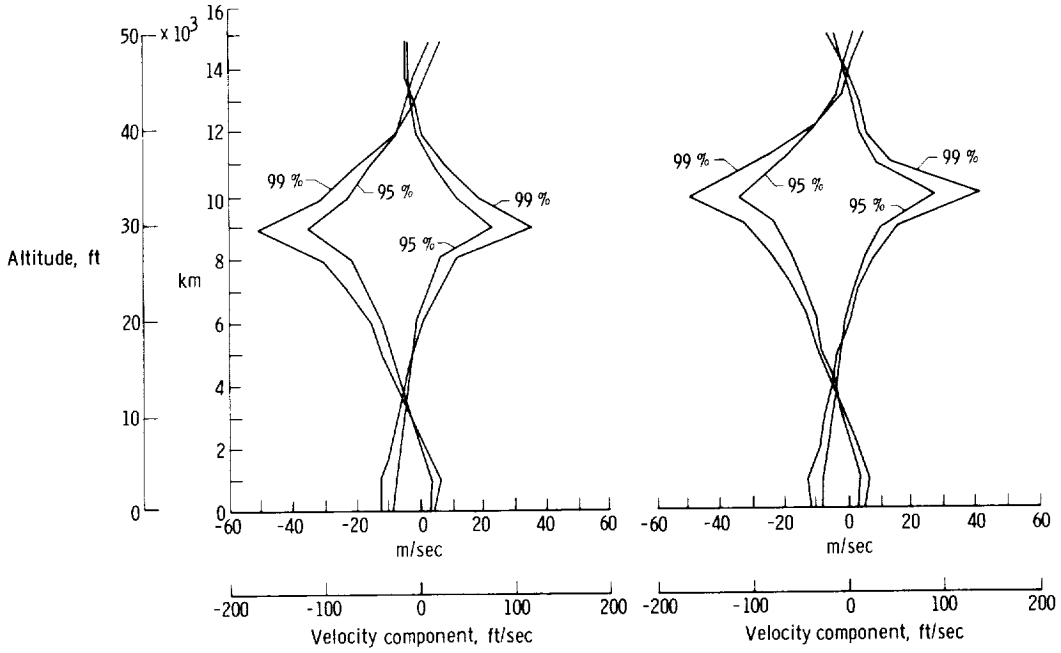

(a) Key level = 9 kilometers.

(b) Key level = 10 kilometers.

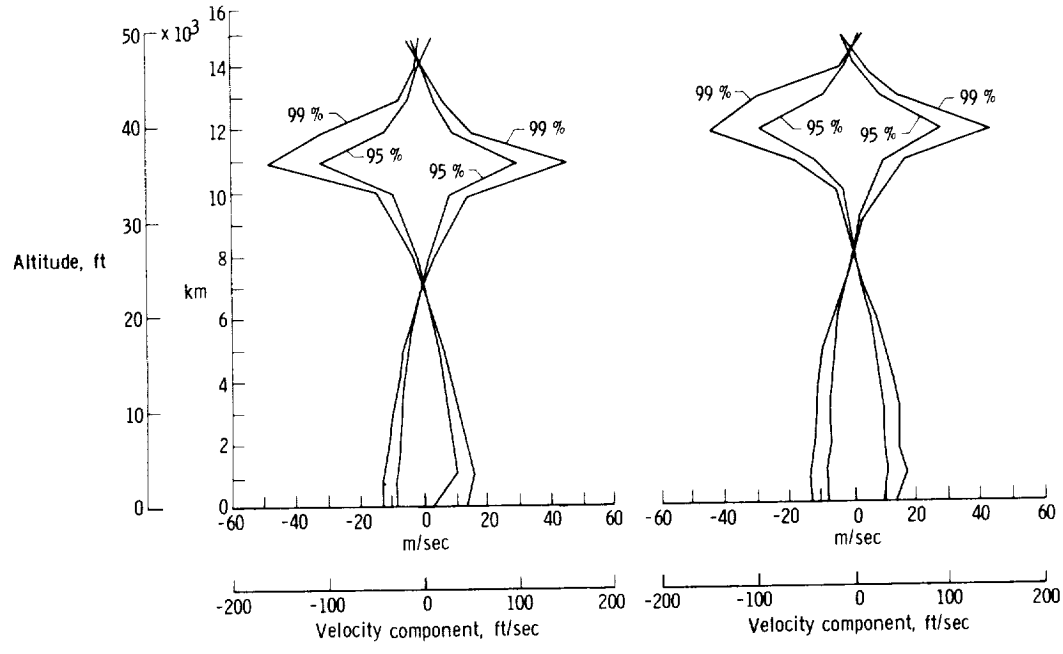

(c) Key level = 11 kilometers.

(d) Key level = 12 kilometers.

Figure 5.- Meridional-component model profiles for month of March at Cape Canaveral for several key levels.

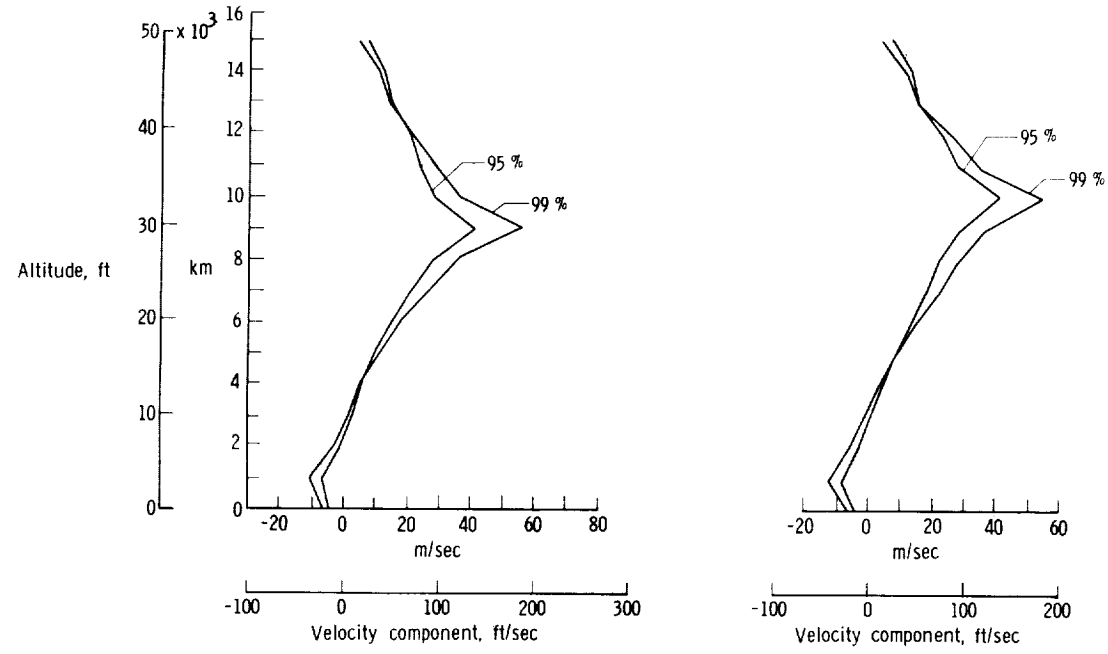

(a) Key level = 9 kilometers.

(b) Key level = 10 kilometers.

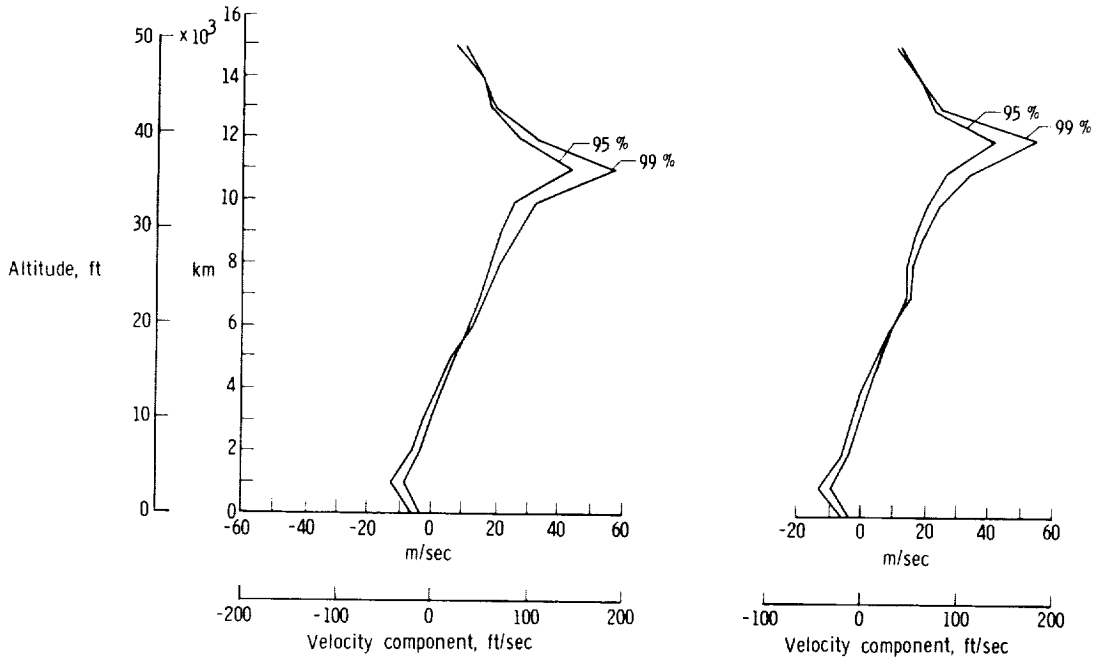

(c) Key level = 11 kilometers.

(d) Key level = 12 kilometers.

Figure 6.- Zonal-component model profiles for month of February at Santa Maria, California, for several key levels.

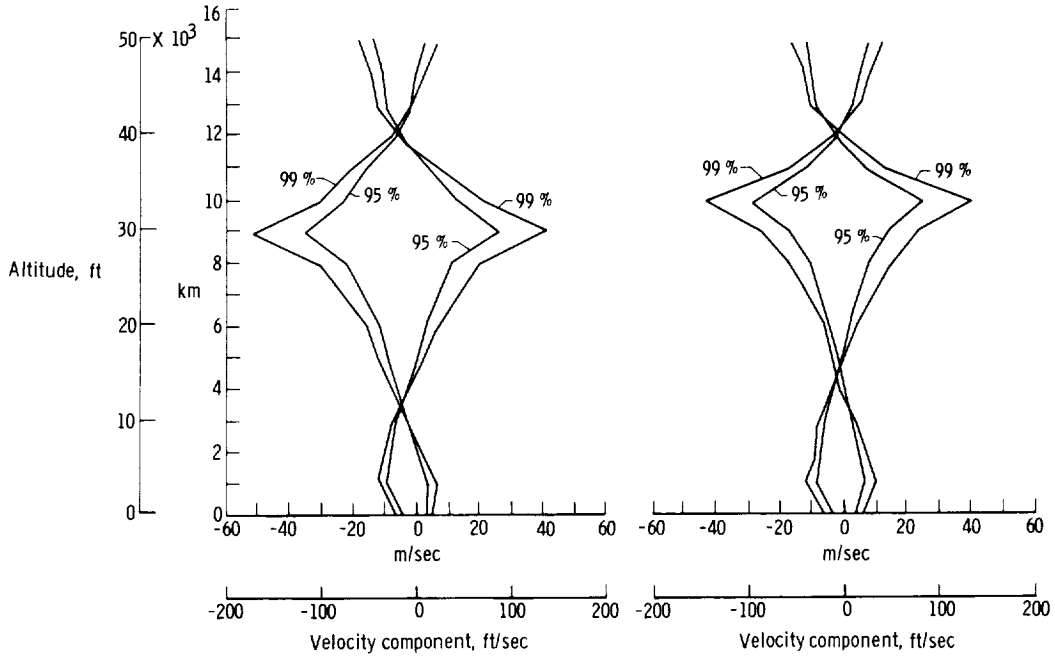

(a) Key level = 9 kilometers.

(b) Key level = 10 kilometers.

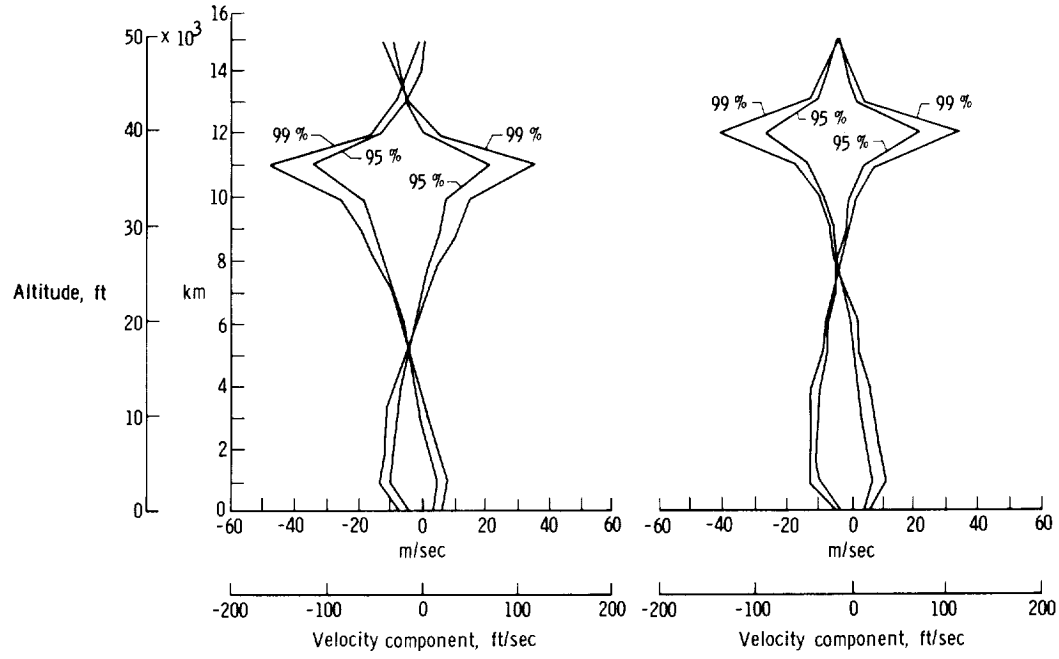

(c) Key level = 11 kilometers

(d) Key level = 12 kilometers.

Figure 7.- Meridional-component model profiles for month of February at Santa Maria, California, for several key levels.

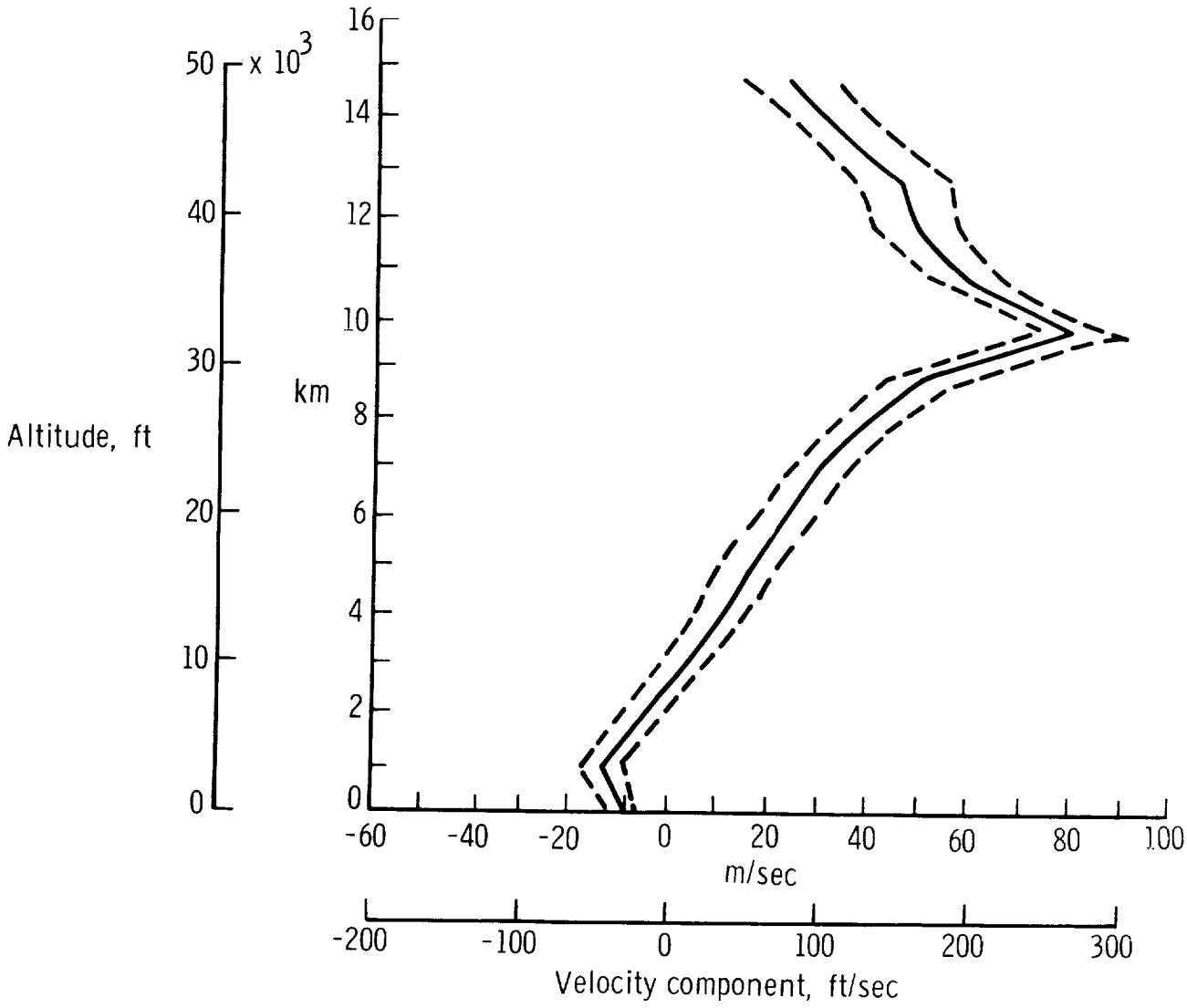

(a) West-to-east component.

Figure 8.- Model profile for month of March at Cape Canaveral for key level of 10 kilometers; 99-percent-level profile with 99-percent confidence limits.

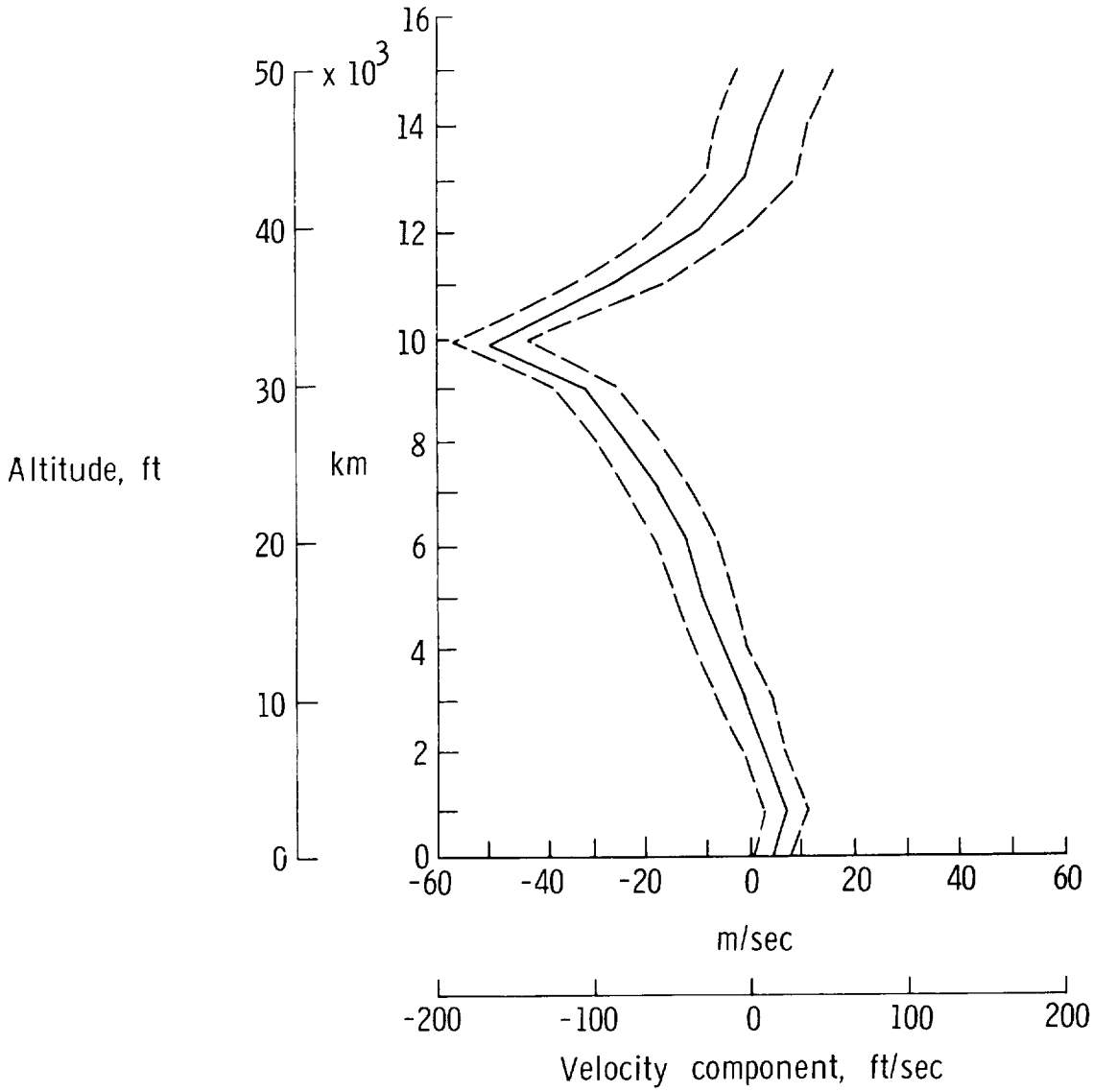

(b) South-to-north component.

Figure 8.- Concluded.

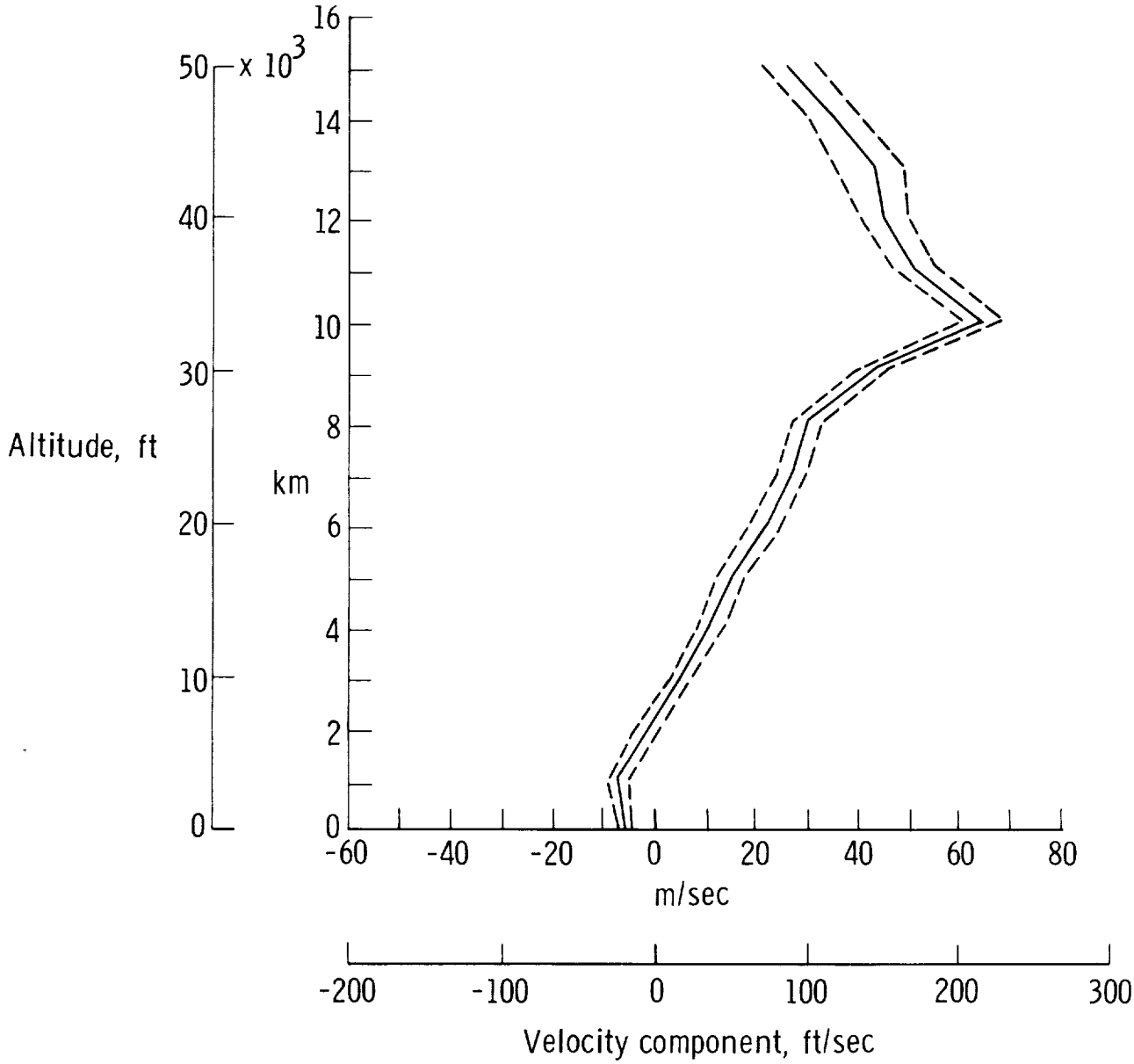

(a) West-to-east component.

Figure 9.- Model profile for month of March at Cape Canaveral for key level of 10 kilometers; 95-percent-level profile with 95-percent confidence limits.

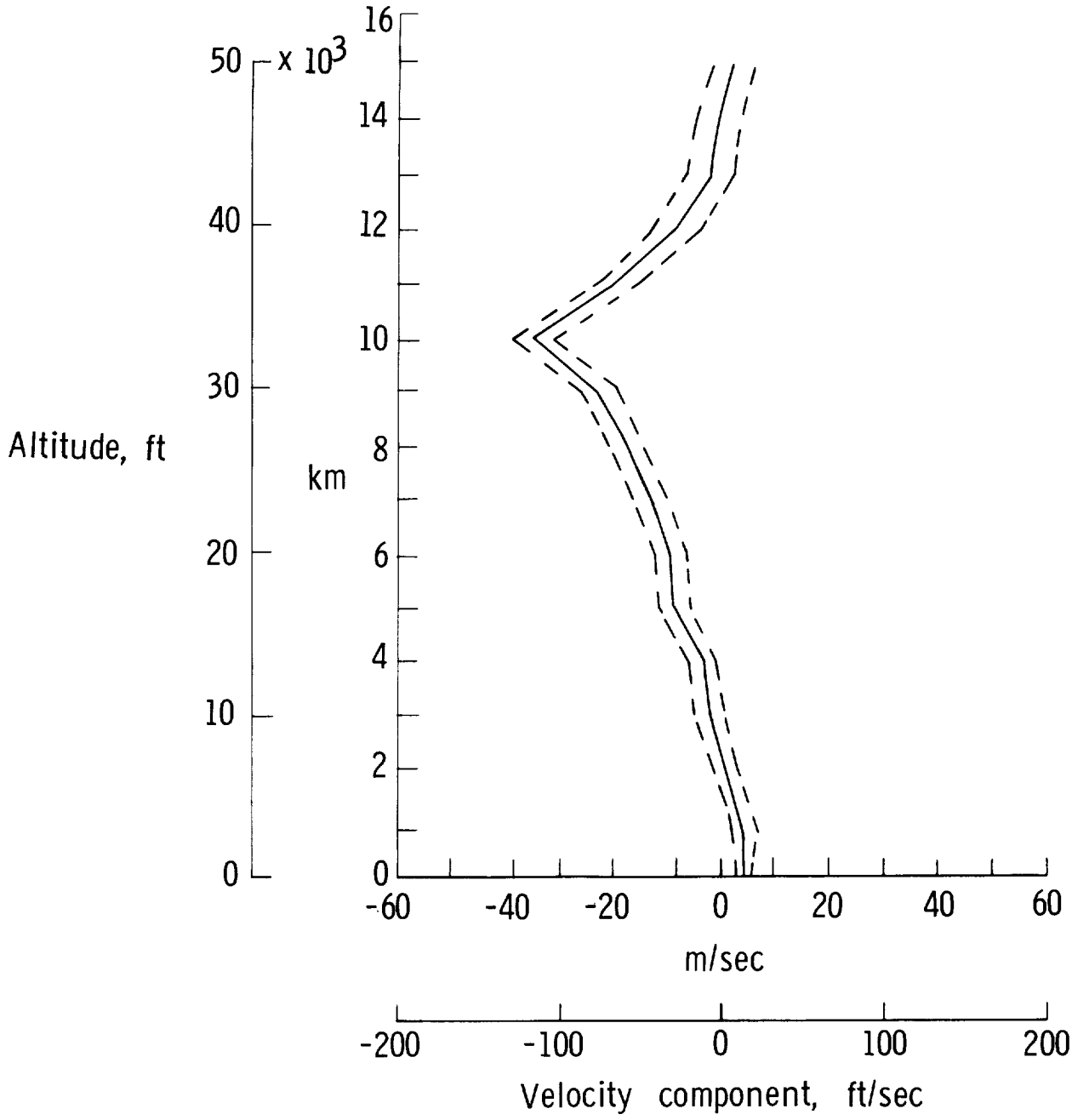

(b) South-to-north component.

Figure 9.- Concluded.